Umbilical cord blood T cells can be isolated and enriched by CD62L selection for use in 'off the shelf' chimeric antigen receptor T-cell therapies to widen transplant options

Christos Georgiadis,[1] Lauren Nickolay,[1] Farhatullah Syed,[1] Hong Zhan,[1] Soragia Athina Gkazi,[1] Annie Etuk,[1] Ulrike Abramowski-Mock,[1] Roland Preece,[1] Piotr Cuber,[1] Stuart Adams,[2] Giorgio Ottaviano[1] and Waseem Qasim[1,2]

[1]UCL Great Ormond Street Institute of Child Health and [2]Great Ormond Street Hospital for Children NHS Trust, London, UK

Correspondence: W. Qasim
w.qasim@ucl.ac.uk

Received: January 20, 2024.
Accepted: July 3, 2024.
Early view: July 11, 2024.

https://doi.org/10.3324/haematol.2024.285101

Abstract

Umbilical cord blood (UCB) T cells exhibit distinct naïve ontogenetic profiles and may be an attractive source of starting cells for the production of chimeric antigen receptor (CAR) T cells. Pre-selection of UCB-T cells on the basis of CD62L expression was investigated as part of a machine-based manufacturing process, incorporating lentiviral transduction, CRISPR-Cas9 editing, T-cell expansion, and depletion of residual TCRαβ T cells. This provided stringent mitigation against the risk of graft-*versus*-host disease (GvHD), and was combined with simultaneous knockout of CD52 to enable persistence of edited T cells in combination with preparative lymphodepletion using alemtuzumab. Under compliant manufacturing conditions, two cell banks were generated with high levels of CAR19 expression and minimal carriage of TCRαβ T cells. Sufficient cells were cryopreserved in dose-banded aliquots at the end of each campaign to treat dozens of potential recipients. Molecular characterization captured vector integration sites and CRISPR editing signatures, and functional studies, including *in vivo* potency studies in humanized mice, confirmed anti-leukemic activity comparable to peripheral blood-derived universal CAR19 T cells. Machine manufactured UCB-derived T-cell banks offer an alternative to autologous cell therapies and could help widen access to CAR T cells.

Introduction

Chimeric antigen receptor (CAR) T cells can mediate leukemic remission in patients that have otherwise failed conventional treatment.[1] Current authorized products are manufactured from autologous peripheral blood lymphocytes derived from steady-state apheresis, and this requires complex logistics, and time for manufacturing and release of products.[2] The quality and fitness of such products is highly dependent on individual patient variables.[3] Alternative allogeneic sources are being investigated as a starting material, including T cells from HLA-matched hematopoietic stem cell transplant donors,[4,5] or donor-derived virus-specific T cells[6] and non-matched genome-edited donor-derived T cells.[7-10] The latter have been derived from adult volunteer donors, and edited to try and address HLA barriers. Steps have included targeted disruption of TCRαβ expression in combination with HLA class I knockout, alone or in combination with class II inhibition.[11-16] We have previously tested strategies to confer resistance to lymphodepleting serotherapy by editing of CD52 and showed that cells persisted for around four weeks in the presence of alemtuzumab, sufficient time to mediate leukemic clearance.[8,9,17]

Umbilical cord blood (UCB) T cells have distinct ontogenetic origins and may offer enhanced properties of expansion and activation, compared to adult peripheral blood lymphocytes.[18] The specific transcriptional signature of UCB T cells has been affiliated with potent anti-leukemic effects after allogeneic transplantation.[19] Several groups have explored the efficacy of UCB-derived immune cells modified to express CAR in pre-clinical models, and clinical testing of cord-derived natural killer (NK) cells has been underway in patients with B-cell malignancies, with encouraging early data.[20-23] UCB T-cell naïvety and high proliferative capacity warrants their further investigation for CAR T-cell production.[24] Challenges include the limited volume of UCB collections and their high

nucleated red cell and mononuclear cell content which complicates T-cell isolation and processing. CD62L is expressed on almost all UCB T cells and we reasoned that selecting for CD62L could allow T cells to be efficiently isolated from umbilical collections. CD62L generally identifies less-differentiated T cells (naïve and central memory T cells) from effector subsets[25,26] and represents an important homing marker.[27] Importantly, selection by targeting CD62L avoids binding of T-cell receptors or other key activation ligands, and this may be important for downstream activation and transduction steps. T cells are most efficiently transduced while undergoing mitosis and this is generally best achieved through a combination of anti-CD3 and anti-CD28 antibody stimulation. Previously, we generated adult donor CAR19 T cells, with T-cell receptor alpha constant gene (*TRAC*) and *CD52* multiplexed knockouts using lentiviral gene modification of peripheral blood CAR T cells for a phase I clinical trial in children with refractory / relapsed (R/R) B-cell acute lymphoblastic leukemia (B-ALL).[8] These processes were now adopted for 'compliance-ready' machine manufacture of UCB T cells, starting with CD62L$^+$ selection and ending with TCR$\alpha\beta^-$ selection of TCR$\alpha\beta$-depleted CAR19 T cells. Molecular, phenotypic, and functional assessments were undertaken to determine suitability and feasibility of downstream therapeutic applications.

Methods

Manufacture of umbilical cord blood-TT52CAR19

Fresh UCB units were collected under ethical approval from volunteers identified independently by the Nolan transplant registry and tissue typed at St Barts Hospital National Health System (NHS) Trust. A unit was directly attached to the CliniMACS Prodigy device (Miltenyi Biotec). T cells were enriched by automatic red blood cell depletion and CD62L positive selection. The CD62L$^+$ UCB T cells were then activated using MACS GMP TransAct (Miltenyi Biotec) on a modified T-cell transduction (TCT) program and cultured in TexMACS supplemented with 3% human serum (HS) (Life Science Production) and interleukin-2 (IL-2) (Miltenyi Biotec) for 24 hours. The cells were transduced 'on device' with TT52CAR19 lentiviral vector, as previously described.[8] On day 4 post activation, cells were removed from the CliniMACS Prodigy and electroporated with capped, polyadenylated, and uridine-modified SpCas9 mRNA using the Lonza 4D-Nucleofector LV unit. Post electroporation, cells were returned to the CliniMACS Prodigy and cultured at 5% CO_2 37°C until day 11 with timed TexMACS supplemented with 3% HS/IL-2. Programmed media changes with shaking enabled for optimal gas exchange. On day 11, cells underwent automatic TCR$\alpha\beta$ depletion on the CliniMACS Prodigy using an anti-biotin bead kit. The depleted cells were rested overnight in the device and the final drug substance was harvested on day 12 and cryopreserved in 1x10^7 and 2x10^7 doses. Next-generation sequencing (NGS) was used for high-resolution tissue typing of UCB1 (HLA-A*02:01:01, -A*24:02:01, HLA-B*07:02:01, -B*15:01:01, HLA-C*03:03:01, -C*07:02:01, HLA-DRB1*01:02:01, -DRB1*15:01:01, HLA-DRB5*01:01:01, HLA-DQB1*05:01:01, -DQB1*06:02:01, HLA-DPA1*01:03:01, -DPA1*02:01:01, HLA-DPB1*04:01:01, -DPB1*11:01:01, HLA-DQA1*01:01:02, -DQA1*01:02:01) and UCB2 (HLA-A*01:01:01, -A*25:01:01, HLA-B*07:02:01, -B*08:01:01, HLA-C*07:01:01, -C*07:02:01, HLA-DRB1*03:01:01, -DRB1*04:01:01, HLA-DRB3* 01:01:02, HLA-DRB4*01:03:01, HLA-DQB1*02:01:01, -DQB1*03:02:01, HLA-DPA1*01:03:01, HLADPB1*04:01:01, HLA-DQA1*03:01:01, -DQA1*05:01:01) batches (*Online Supplementary Table S1*).

Phenotype, function and molecular characterization

Flow cytometry was undertaken using a BD FACSCanto II (Becton, Dickinson BD Biosciences) at Great Ormond Street Hospital (GOSH) NHS Trust, with additional characterization using a BD LSRII (Becton, Dickinson BD Biosciences), and analysis using FlowJo v10 (TreeStar Inc.).

Quantification of 'on-target' and 'off-target' editing effects and translocations

Polymerase chain reaction (PCR) amplicons of target genomic DNA were Sanger sequenced and non-homologous end joining (NHEJ) events analyzed using Inference of CRISPR Edits (ICE) protocols (https://ice.synthego.com/#/). 'On-target' and 'off-target' sites were informed by previous Digenome-seq studies[7,28] (*Online Supplementary Table S2*) and libraries subjected to paired-end NGS using MiniSeq (Illumina), as previously described.[29-31] Droplet digital PCR (ddPCR) was used to quantify predicted translocations between chromosomes 14q (TRAC) and 1p (CD52) loci and analyzed using Quantasoft (BioRad) (*Online Supplementary Table S2*) (BioProject accession n.: PRJNA1061060).

In vitro cytotoxicity assay

In vitro cytotoxic function of UCB-TT52CAR19 GMP1 (UCB1) and UCB-TT52CAR19 GMP2 (UCB2) or peripheral blood leukapheresis (PBL)-derived batches alongside controls was quantified by co-culture with chromium (^{51}Cr) loaded CD19$^+$ Daudi and CD19$^+$ or CD19$^-$ SupT1 cells for four hours at 37°C at increasing effector-to-target (E:T) (0.16:1-20:1 where a 1:1 E:T used 5x10^4 of each group) ratios and ^{51}Cr release was quantified using a Wallac MicroBeta TriLux microplate scintillation counter.

In vivo studies

In vivo function was assessed in non-obese diabetic (NOD) / severe combined immunodeficiency (SCID)/γc (NSG) mice inoculated intravenously by tail vein injection with 0.5x10^6 CD19$^+$ Daudi tumor cells expressing enhanced

green fluorescence protein (eGFP) and luciferase, followed by 5x10^6 UCB1-, UCB2- or PBL-derived effectors and non-edited or non-transduced controls after four days. Serial bioluminescence imaging using an IVIS Lumina III In Vivo Imaging System (PerkinElmer, Living Image® version 4.5.5) was used to track leukemia inhibition for up to four weeks.

Statistical analysis

Statistical analyses were performed with Prism (GraphPad) using unpaired *t* test or ANOVA where indicated. Values from 3 or more samples are presented as mean with Standard Error of Mean (SEM). $P<0.05$ was considered statistically significant.

Results

Machine mediated CD62L$^+$ T-cell enrichment and engineering of umbilical cord blood donations

Banks of UCB-TT52CAR19 (UCB1 and UCB2) were manufactured from 2 fresh, unrelated volunteer donor, cord blood collections using a CliniMACS Prodigy device (Figure 1, *Online Supplementary Table S1*). One key hurdle in handling and manipulating UCB donations is the high number of nucleated red cells. We investigated CD62L$^+$ T-cell enrichment by CD62L selection using magnetic bead positive selection. A yield of >4x10^7 CD62L$^+$ cells was set as a starting material minimum before activation with anti-CD3/CD28 Transact reagent and lentiviral transduction. We found that this was readily achieved, with the UCB units yielding: 1.33x10^8 (UCB1) and 0.96x10^8 (UCB2) CD62L$^+$ lymphocytes from donations of 1.2x10^9 and 8.2x10^8 MNC, respectively (Figure 2A, B, *Online Supplementary Table S3*). Using a multiplicity of infection of around 5, transduction efficiencies of 67% (UCB1) and 74% (UCB2) were achieved (Figure 2C, *Online Supplementary Figure S1*).

Next, electroporation was performed 'off-device' using a Lonza LV for transient delivery of SpCas9 mRNA. Flow cytometry on day 7 found residual TCR$\alpha\beta^+$ (UCB1 34.6%; UCB2 35.4%) and CD52$^+$ (UCB1: 35.4%; UCB2: 30.2%) (Figure 2C, *Online Supplementary Figure S1*). 'On-device' prodigy expansion for three days was followed by automated bead-mediated depletion of residual TCR$\alpha\beta^+$ T cells with UCB1 exhibiting 0.2% and UCB2 0.3% TCR$\alpha\beta^+$ cells at the end of processing. Simultaneously, the CAR$^+$ fraction increased to >80% by the end of production as a result of coupling effects of editing and transduction in the TT52CAR19 configuration. Yields of 9.1x10^8 and 5.5x10^8 cells in total were achieved for UCB1 and UCB2, respectively. The product was cryopreserved in 1 mL aliquots of 1x10^7 (x 20 vials for each UCB1 and UCB2 batch) and 2x10^7 (x 10 vials for each UCB1 and UCB2 batch) total cells in individual vials and stored at < -130°C (Table 1). Western blot and ELISA did not detect presence of Cas9 at the end of production (*Online Supplementary Figure S2*).

Phenotype and molecular characterization of umbilical cord blood-TT52CAR19

At the end of production, >80% of cells were CD45RA$^+$CD62L$^+$ (*Online Supplementary Figure S3*) with 85-92% CAR expression. Transduction was corroborated by proviral copy number by qPCR (UCB1 VCN: 2.7; UCB2 VCN: 4.0 copies/cell). 'On-target' genome editing signatures of NHEJ were verified by quantification of insertions / deletions (indels) at TRAC (UCB1: 76%; UCB2: 59%) and CD52 (UCB1: 58%; UCB2: 51%) loci by ICE analysis of Sanger sequence traces (Figure 3A, *Online Supplementary Figure S4A*). Targeted ddPCR quantification for NHEJ at these sites provided corroboration (TRAC: 65%, 47%; CD52: 73%, 38%) (Figure 3B, *Online Supplementary Fig-*

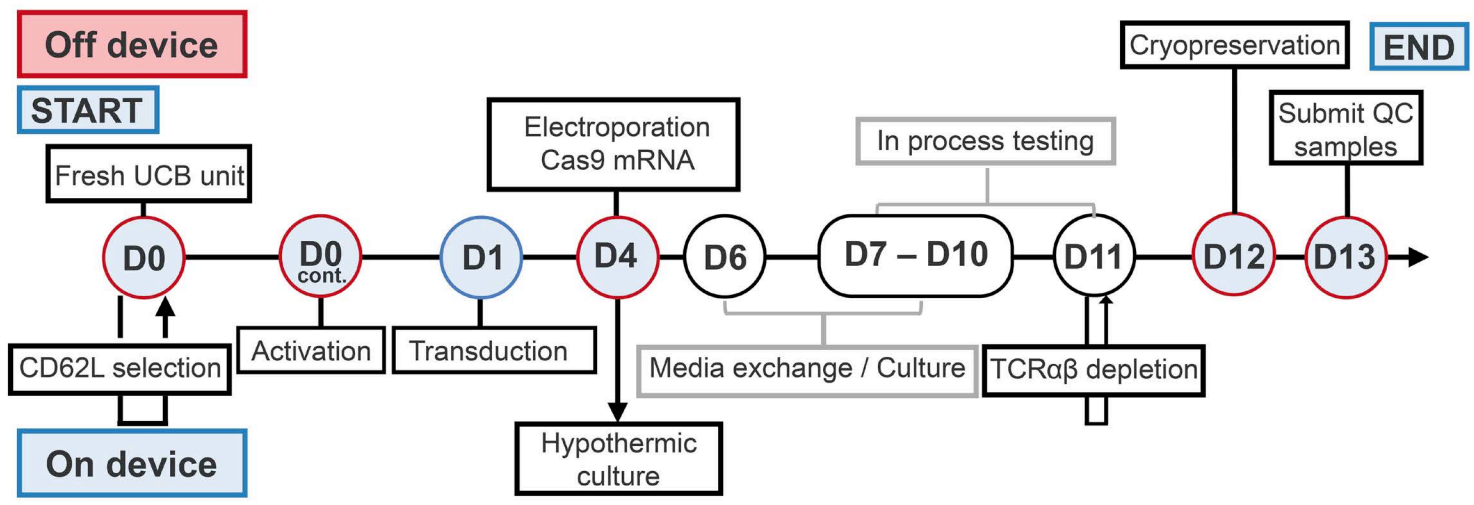

Figure 1. Schematic timeline for Good Manufacturing Practice manufacturing of TT52CAR19 cell banks from umbilical cord blood starting material. Fresh umbilical cord blood (UCB) units were enriched for lymphocytes by CD62L$^+$ magnetic bead positive selection and activated on day 0 (D0). T cells were transduced 24 hours later (D1) with TT52CAR19 vector and electroporated on day 4 (D4) with SpCas9 mRNA. On day 11 (D11), cells underwent automated TCR$\alpha\beta$ T-cell depletion. After this step, the final cell product was harvested and cryopreserved in therapeutic doses. Steps itemised below the timeline were performed on a Miltenyi Prodigy and are shown as 'On device',, with the remaining items (above the timeline) undertaken 'Off device'. cont.: continued; QC: quality control.

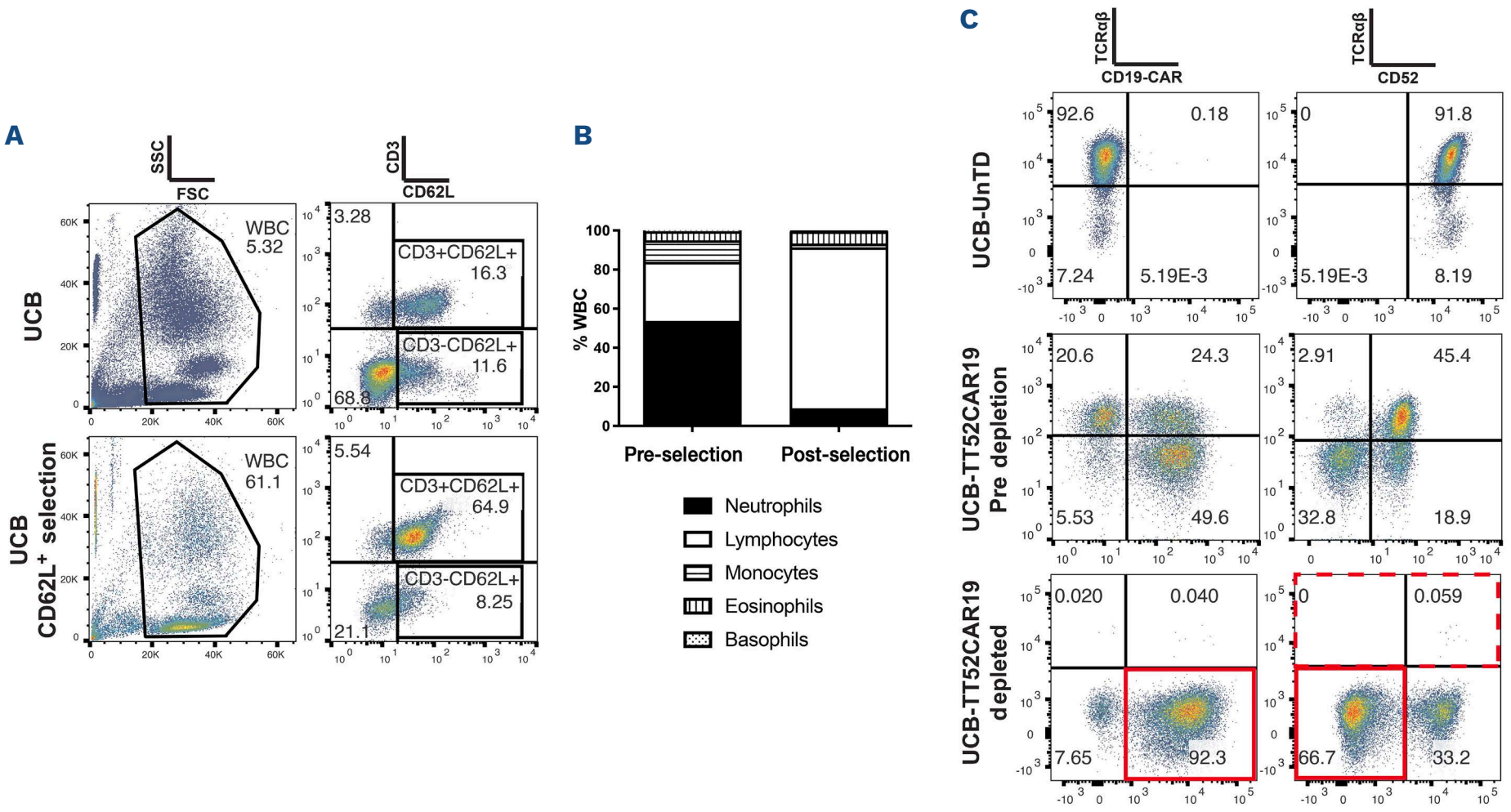

Figure 2. Whole umbilical cord blood CD62L selection using the CliniMACS Prodigy and TT52CAR19 batch manufacture. (A) Umbilical cord blood (UCB) cells pre- and post-CD62L$^+$ selection using the CliniMACS Prodigy demonstrates enrichment of CD3$^+$ T cells. (B) Cord blood cells from UCB donors (N=4) were analyzed by Sysmex pre- and post-CD62L selection using the CliniMACS Prodigy. (C) Flow cytometric T-cell transduction and knockout analysis of UCB-TT52CAR19 GMP1 (UCB1) cell bank. UCB-TT52CAR19 cells were stained before and after up to 2 rounds of magnetic TCR$\alpha\beta$ depletion alongside untransduced (UnTD) cells or non-edited UCB-TT52CAR19 TCR$^+$ cells. Transduction efficiency was measured by quantifying transgene expression using F(ab')2, and CRISPR-Cas9-mediated protein knockout was determined through staining for TCR$\alpha\beta$ and CD52. FSC: forward scatter; WBC: white blood cells; CAR: chimeric antigen receptor.

ure S4B). Lentiviral integration was mapped by LM-PCR with the top 10 most frequent sites presented in Figure 4 and *Online Supplementary Figure S5*.

End of production screening for aberrant DNA breaks

Karyotype analysis reported normal G-band analysis with no detection of chromosomal aberrations. Further investigations by FISH analysis found no evidence (within the limits of the probe set) of TRAD rearrangements in 197/200 cells (98.5%). Predictable translocation events were investigated (Figure 5A, *Online Supplementary Figure S6A*) for 4 predicted recombinations (C1-C4) involving 14p (TRAC locus) and 1q (CD52 locus), and low frequency events (<1.0%) were quantified by ddPCR for each reaction, with 0.64% (UCB1) and 0.73% (UCB2) in total quantified over the 4 reactions.

Previously, Digenome-Seq analysis had informed the design of screening for 'off-target' guide-dependent editing for the TT52CAR19 vector system. An abbreviated form of the screen was now applied at the 6 highest scoring genomic sites (Figure 5B, *Online Supplementary Figure S6B*). Targeted NGS found modification frequencies at these sites of <0.5% in both batches, whereas 'on-target' NHEJ events were quantified as 65% and 51% at the TRAC locus, and 73% and 17% at the CD52 locus for UCB1 and UCB2, respectively.

Table 1. Umbililcal cord blood-TT52CAR19 GMP1 and GMP2 end of manufacture batch specifications.

	UCB-TT52CAR19-GMP1 (UCB1)	UCB-TT52CAR19-GMP2 (UCB2)
Viability, 7AAD,[1] %	96.2	99.8
CAR19 transduction efficiency, %	88.7	82.8
Purification	0.2% CD45$^+$TCR$\alpha\beta^+$ cells	0.3% CD45$^+$TCR$\alpha\beta^+$ cells
Sterility, BACTEC[2]	No growth	No growth
Sterility, gram stain	No organisms seen	No organisms seen
Mycoplasma	None detected	None detected
Endotoxin, EU/mL	<1.0	<1.0
Yield	906x10^6	546x10^6

UCB: umbilical cord blood. [1]7-aminoactinomycin D (7AAD) used as fluorescent probe of non-viable cell exclusion. [2]BACTEC blood culture media for detection of aerobes, anaerobes, yeast, fungi, and mycobacteria; CAR: chimeric antigen receptor; TCR: T-cell receptor.

A

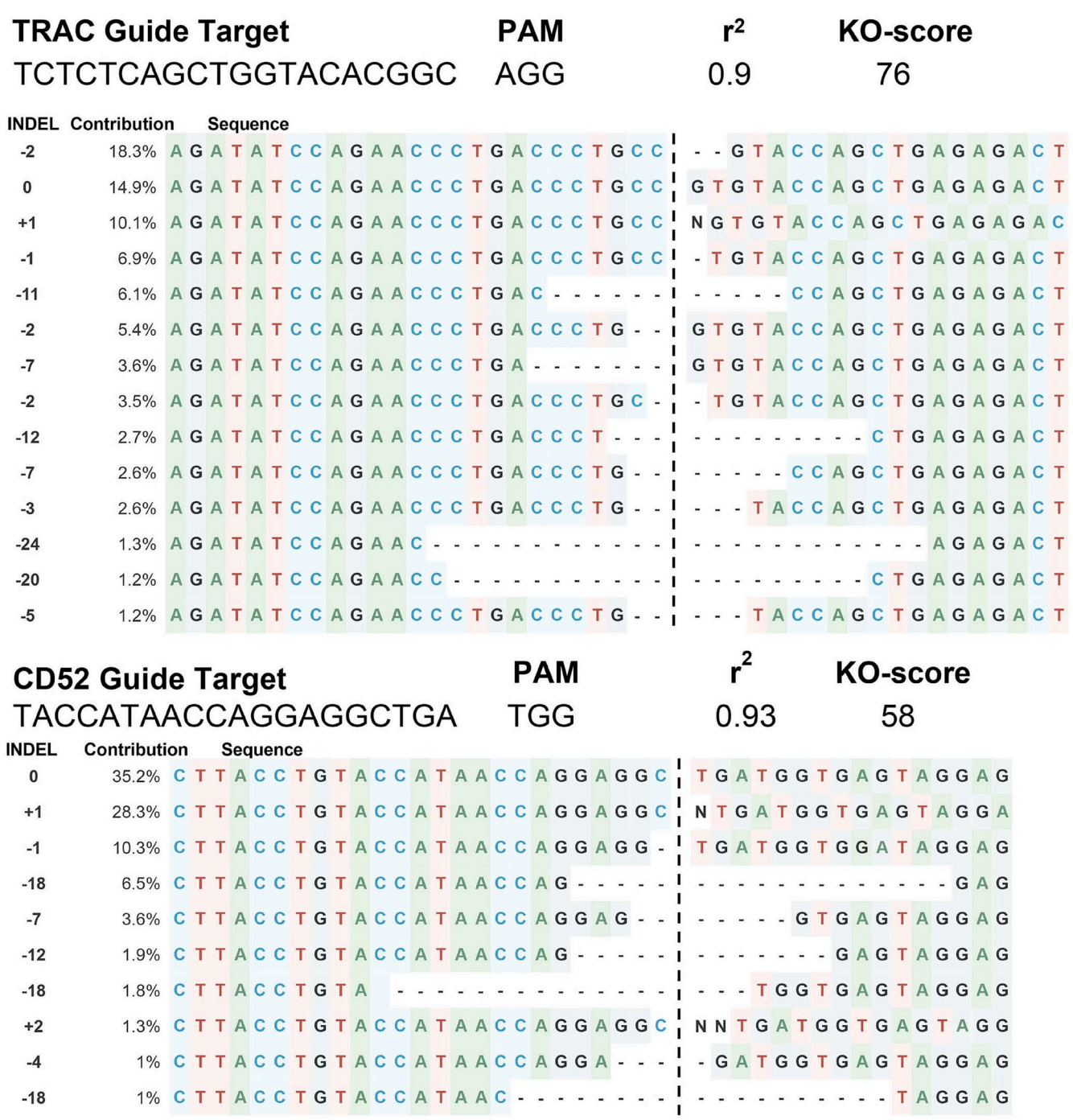

B

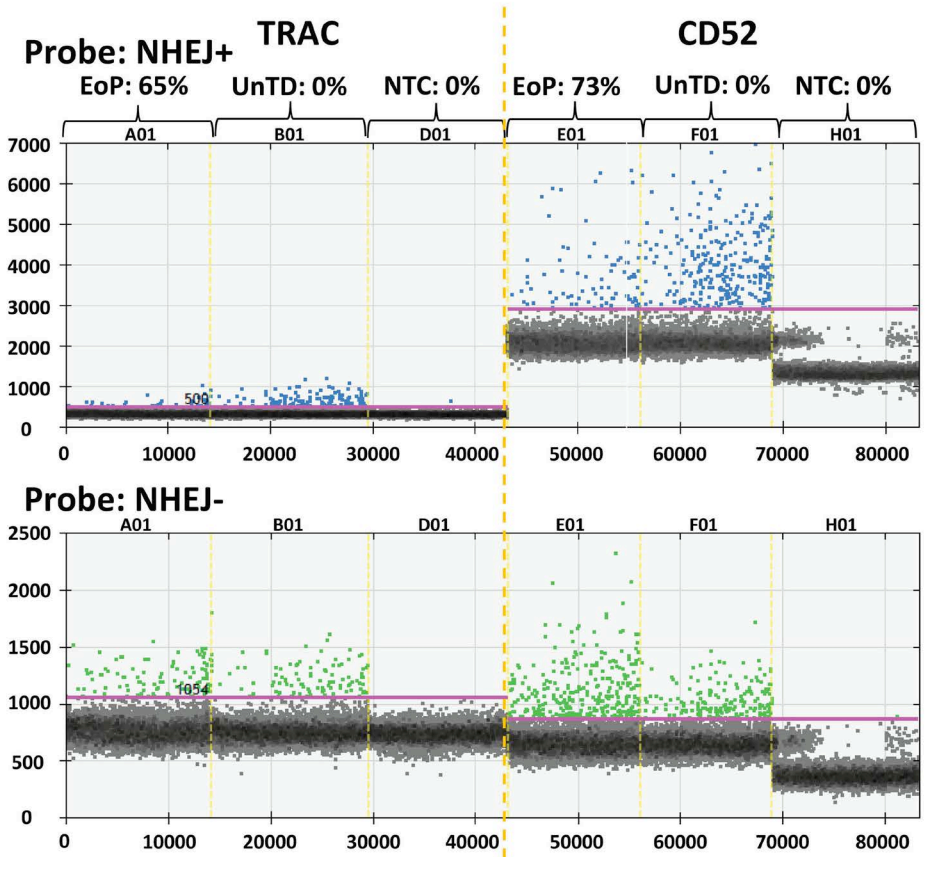

Figure 3. Molecular characterization of 'on-target' CRISPR-Cas9-mediated cleavage. (A) ICE analysis of Sanger sequence traces identified indels as signatures of NHEJ at the TRAC locus and at the CD52 target site. (B) Quantification of indels by ddPCR at both the TRAC and CD52 sites using separate probes, one specific to the predicted NHEJ region (NHEJ$^+$) and a second outside the NHEJ region (NHEJ$^-$). EoP: end of production; UnTD: non-transduced controls; NTC: non-treated control.

Functional studies of umbilical cord blood-TT52CAR19 cells

The potency of each UCB-TT52CAR19 batch was assessed against ^{51}Cr labeled CD19$^+$ Daudi cells and CD19$^+$ or CD19$^-$ SupT1 cells (Figure 6A, *Online Supplementary Figure S7A-C*). Specific lysis was demonstrated across a range of E:T ratios compared to untransduced (UnTD) cells (***P*<0.01) with results comparable to TT52CAR19 products generated from adult PBL (Figure 6B). In addition, cytokine production was measured following a 1:1 co-culture with CD19$^+$ Daudi cells and CD19$^+$ or CD19$^-$ SupT1 cells (Figure 6C, *Online Supplementary Figure S7D-F*) and secretion of cytokines IFN-γ, TNF-α, IL-4 and IL-2, compared to PBL-derived TT52CAR19 cells (Figure 6D).

A chimeric human : murine xenograft model of B-cell malignancy was used to assess *in vivo* function of UCB-TT52CAR19 cells (Figure 7A). NSG mice were engrafted with 5x10^5 CD19$^+$eGFP$^+$Luciferase$^+$ Daudi cells and 5x10^6 UCB-TT52CAR19 effectors were infused four days later. Serial bioluminescence imaging over a 4-week period showed rapid disease progression in mice receiving UnTD cells, whereas mice treated with UCB-TT52CAR19 cells exhibited significantly reduced tumor signal and inhibition of disease throughout the monitoring period: UCB-UnTD GMP1 *versus* UCB-TT52CAR19 GMP1 (UCB1), *P*<0.0001; UCB-UnTD GMP2 *versus* UCB-TT52CAR19 GMP2 (UCB2), (*P*<0.0001) (Figure 7B, C, *Online Supplementary Figure S8*). Anti-leukemic activity was similar to animals treated with PBL TT52CAR19 effector batches (UCB1 *vs.* PBL, *P*=0.975; UCB2 *vs.* PBL, *P*=0.986).

Rank	Gene name	Frequency, %	Location
Top1	EIF5A	0.069	17-7304911
Top2	SPIN4	0.061	X-63353021
Top3	DNAJC7	0.06	17+41988746
Top4	ATP11B	0.058	3+182905619
Top5	LRMP	0.056	12+25058347
Top6	RNASET2	0.055	6-166958978
Top7	APOO	0.055	X-23850789
Top8	FAM222B	0.054	17+28801017
Top9	MLXIP	0.054	12-122135898
Top10	CEP97	0.053	3-101760227
#All other mapp. IS	14106	99.425	

Eq count 10 strongest	564
Count all other mapp .IS	97465
Total seq counts used	98029

Figure 4. Integration site analysis. Ligation-mediated polymerase chain reaction (LMPCR) detection and quantification of vector integration sites (IS) where the top 10 most frequent sites comprised <0.1% of integrants.

Discussion

Despite breakthroughs using autologous CAR T cells, there are notable hurdles to wider access to CAR therapies. Alternative 'off-the-shelf' CAR T-cell banks suitable for multiple patients could ultimately reduce costs and avoid delays. Donor peripheral blood T cells have been successfully used to generate 'universal' allogeneic CAR T cells. To overcome HLA mismatching, genome editing has been used to address the risk of GvHD by disrupting TCRαβ and incorporating TCRαβ depletion steps. Mitigations against host-mediated rejection have included CD52 disruption to confer advantage in the presence of alemtuzumab. Alternatively, direct disruption of HLA molecules, through editing of B_2M to prevent expression of HLA class I and class II by targeting transcription factors are under investigation, and approaches to creating allogeneic universal banks have been recently reviewed.[32,33] Umbilical cord donations may offer alternative sources of immune cells with potentially advantageous immunological properties. UCB-derived NK cells have been of interest for their capacity to be used without HLA matching.[22] Trials have been underway for UCB NK cells transduced to express CAR19 and IL-15 to support antigen-driven expansion.[21] In a phase I clinical trial (clinicaltrials.gov identifier: 03056339), the first patients have exhibited anti-leukemic activity without severe toxicities.[20] Could cord blood T cells offer favorable expansion, persistence or longevity compared to adult PBL? The importance of starting T-cell subsets for CAR T-cell manufacturing has been reported in pre-clinical and clinical studies.[34,35] When peripheral blood selected naïve/stem cell memory (N/SCM) CD62L$^+$ CAR T cells were compared to unselected T cells, they appeared to provide better expansion and persistence, and anti-leukemic responses in chimeric mice.[36] One important caveat has been the interpretation of flow-based phenotyping using conventional memory/naïve panels which may not be straightforward after activation and transduction with CAR with different activation domains. Previous studies have included UCB units transduced with a retroviral vector incorporating CAR19 and an IL-12 transgene, which exhibited central memory phenotypes by the end of manufacture and expression of cytotoxic effector proteins granzyme B and IFNγ.[23] Potent anti-leukemic clearance in a preclinical mouse model of B-ALL was reported. In other work, cord blood units expressing anti-CD123 CAR T cells retained a less differentiated phenotype after activation and transduction, with anti-leukemic activity in *in vitro* and *in vivo* models.[37] We reasoned that CD62L could be an ideal selection target of cord T cells for manufacturing CAR T cells. In addition, a key hurdle in manufacturing from cord blood involves distinguishing T cells from other mononuclear cells. Cord blood is rich in nucleated red cells, causing difficulties in enumeration and analysis, and creating challenges for setting optimal culture and

transduction conditions. Pre-selection using anti-CD62L magnetic bead enrichment allowed efficient automated enrichment of cord T cells ahead of activation. The process could be readily incorporated into a CliniMACS Prodigy matrix, and, with compliant reagents already available, included in established transduction and editing processes.

Overall, we found that CD62L^{+} cord CAR19 T cells exhibit

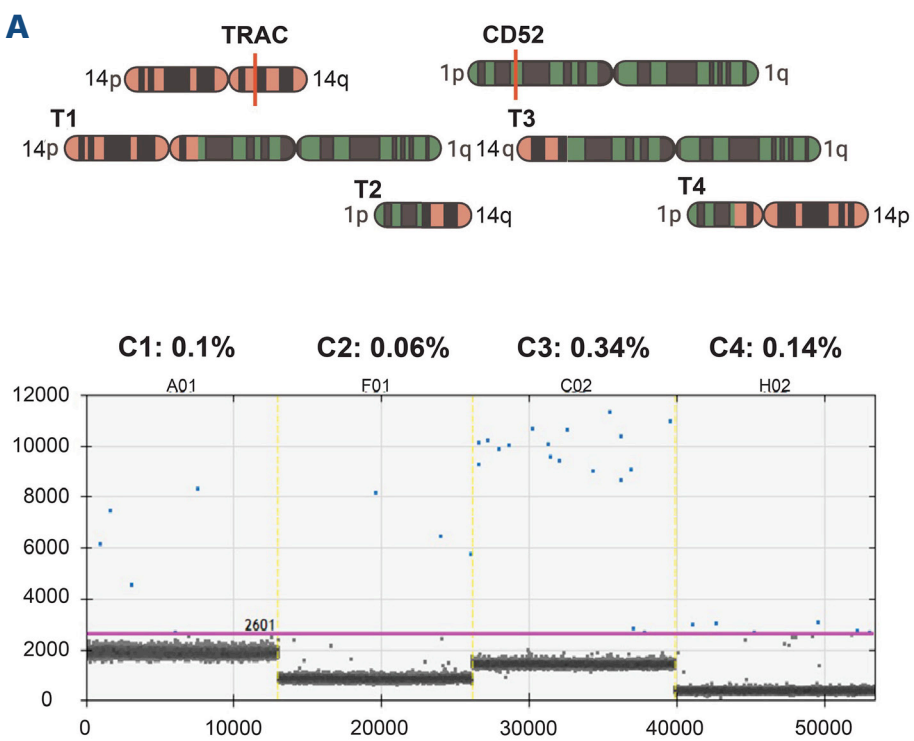

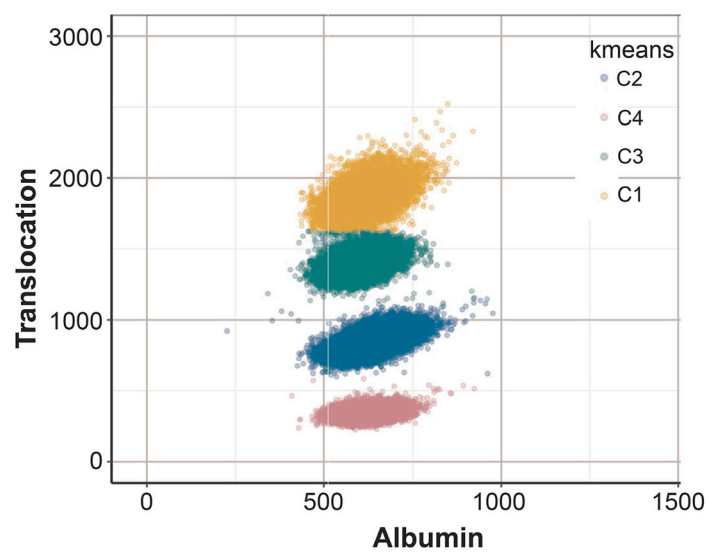

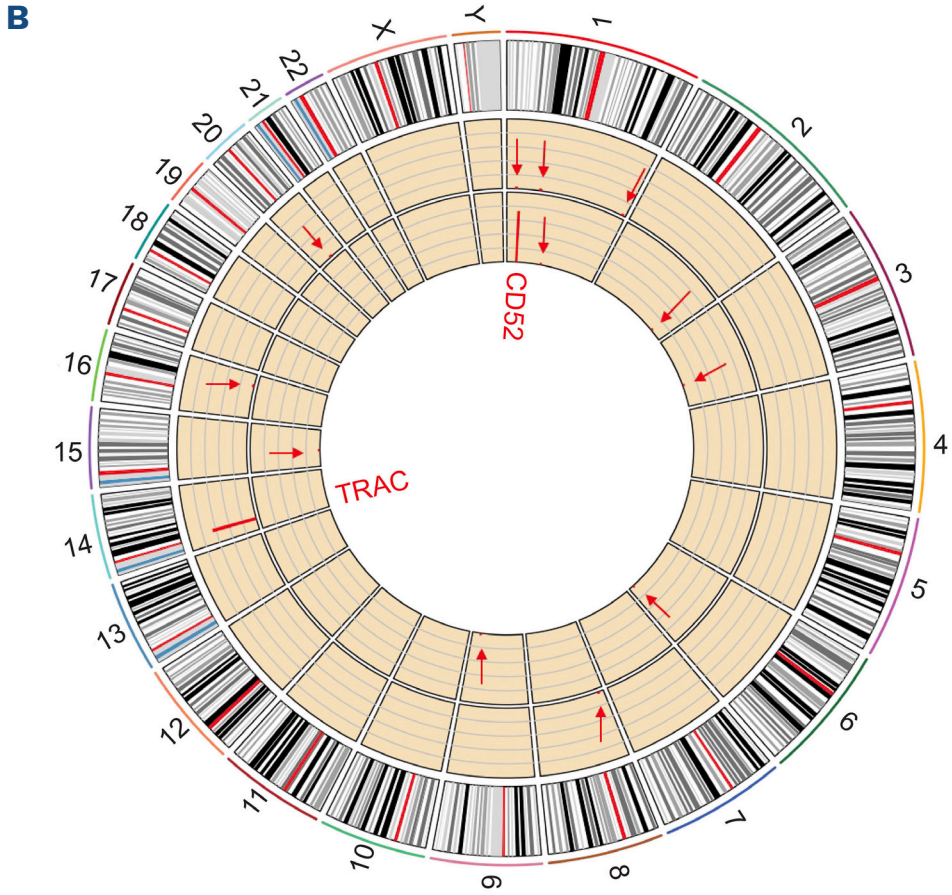

TRAC

Index	Chromosome	ChromStart	ChromEnd	Mutant Frequency
TRAC-01	chr14	23016465	23016487	65
TRAC-02	chr8	10627242	10627255	0.03
TRAC-03	chr1	68621798	68621815	0.03
TRAC-04	chr1	19612375	19612394	0.05
TRAC-05	chr1	242872248	242872256	0.15
TRAC-06	chr20	31622178	31622197	0.06
TRAC-07	chr16	66528021	66528030	0.03

CD52

Index	Chromosome	ChromStart	ChromEnd	Mutant Frequency
CD52-01	chr1	26644530	26644550	73
CD52-02	chr9	118431460	118431490	0.04
CD52-03	chr15	45497075	45497095	0.02
CD52-04	chr1	95875500	95875515	0.03
CD52-05	chr2	207739015	207739040	0.02
CD52-06	chr3	135905235	135905255	0.04
CD52-07	chr6	156954690	156954710	0.03

Figure 5. Detection for translocation and 'off-target' CRISPR-Cas9-mediated cleavage events. (A) (Top left) Droplet Digital polymerase chain reaction (ddPCR) was used for the detection and quantification of possible translocations after 'on-target' DNA scission. Four predicted recombination events (C1-C4) are presented in the schematic with TRAC (Chr14q) (red), CD52 (Chr1p) (green), and SpCas9 cleavage site (red line). (Right) Colours (yellow, green, blue, magenta) discriminate 4 possible translocations. (Bottom left) Low frequency translocation events (blue dots) C1-C4 arising between the edited TRAC and CD52 loci. Cumulative events for all 4 possible events were <1%. (B) (Left) Circos plot with verification of quantification using targeted NGS across the 6 highest scoring predicted 'off-target' sites. TRAC-01 (solid red line marking locus in outer yellow circle), CD52-01 (solid red line marking inner yellow circle), and at predicted 'off-target' sites TRAC-02-TRAC-07 (red arrows marking outer yellow circle) and CD52-02-CD52-07 (red arrows marking inner yellow circle). (Right) Table shows that negligible 'off-target' events were detected for both the TRAC and CD52 guides.

expansion and anti-leukemic activity *in vitro* and *in vivo* comparable to control peripheral blood genome edited CAR19 T-cell products that have already been investigated in the clinic.[8] Cord collection offers a further advantage in allowing ready access to a broad range of HLA haplotypes with tolerance for one or 2 antigen mismatches. Ultimately, the risk of host-mediated rejection could be mitigated using batches of cells generated from donors homozygous for common HLA haplotypes. This could help avoid the need for intensive lymphodepletion currently applied to address barriers caused by HLA mismatches. It has been estimated that a large proportion of European populations could be partly or fully HLA matched to 'off the shelf' cord blood banks derived from around 150 different donors.[38] Alternatively, as it is also now feasible to selectively remove mismatched HLA molecules from partially matched donations, a smaller pool of banked donations selectively retaining matched HLA molecules may prove sufficient.[39]

In summary, UCB T cells can be isolated and enriched by CD62L selection and are amenable to machine-based gene modification, both using lentiviral vectors and by

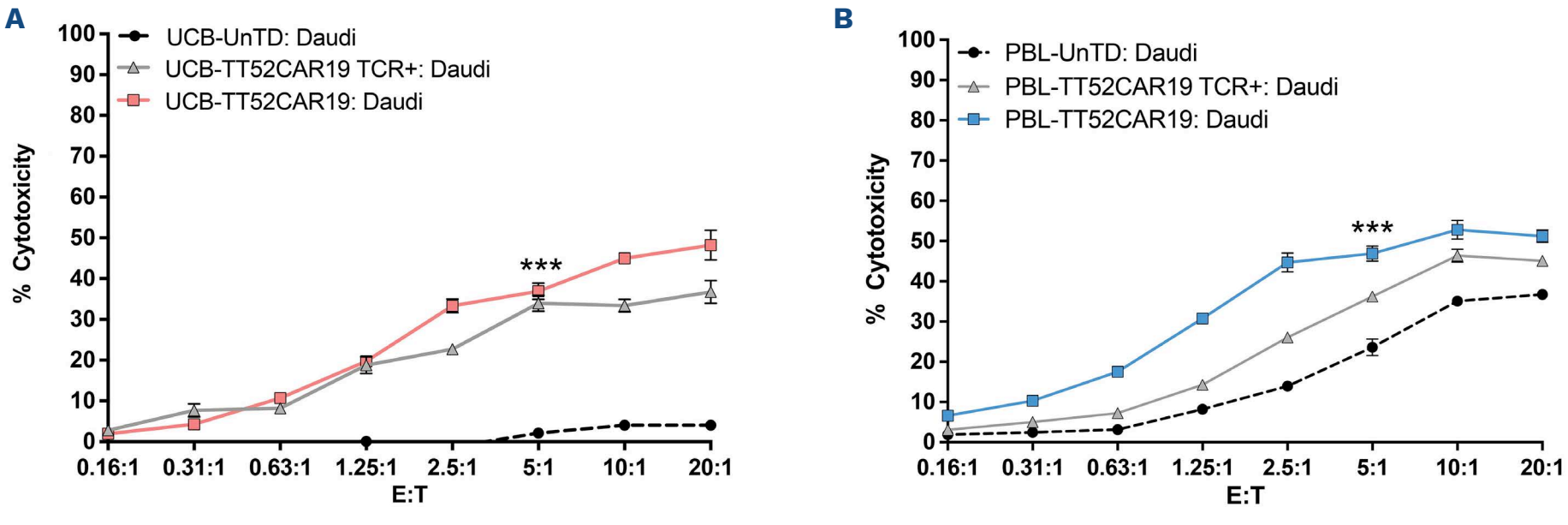

Figure 6. *In vitro* killing potential and cytokine production of umbilical cord blood-TT52CAR19 cells against CD19⁺ targets. *In vitro* cytotoxicity of umbilical cord blood (UCB)-TT52CAR19 GMP1 (UCB1) cell bank compared to respective UCB-TT52CAR19 transduced but not edited (UCB-TT52CAR19 TCR⁺) or non-transduced (UnTD) controls (A) or PBL-TT52CAR19 effectors and respective controls (B) when measured by ^{51}Cr chromium release of labeled CD19⁺ Daudi cells following four hours of co-culture at incremental effector (E) : target (T) ratio. Cell co-cultures ranged from $1x10^5$: $5x10^4$ (at E:T of 20:1) to $8x10^2$: $5x10^4$ (at E:T of 0.16:1). Effector responses were considered successful if ≥50% lysis was detected compared to UnTD controls at E:T cell ratios between 1.25:1 and 5:1. Error bars represent Standard Error of Mean (SEM), N=3 replicate/wells. *In vitro* target specific cytokine secretion of UCB-TT52CAR19 GMP1 cell bank (UCB1), and respective UCB-TT52CAR19 TCR⁺ or non-transduced (UnTD) controls after co-culture with CD19⁺ Daudi cells overnight (C). Cytokine release also quantified for PBL-TT52CAR19 effectors and respective PBL-TT52CAR19 TCR⁺ and UnTD control at 1:1 E:T ($1.25x10^5$ of each effector and target cells) co-cultures with CD19⁺ Daudi cells (D). The presence of cytokines in the co-culture supernatant was measured by cytokine bead array and levels >50 pg/mL were considered positive responses. Significance was calculated between UCB-TT52CAR19 GMP1 (UCB1) or PBL-TT52CAR19 banks and respective UnTD controls. *P<0.05, **P<0.01, ***P<0.001, ****P<0.0001 by t test. Error bars represent SEM, N=3 replicates.

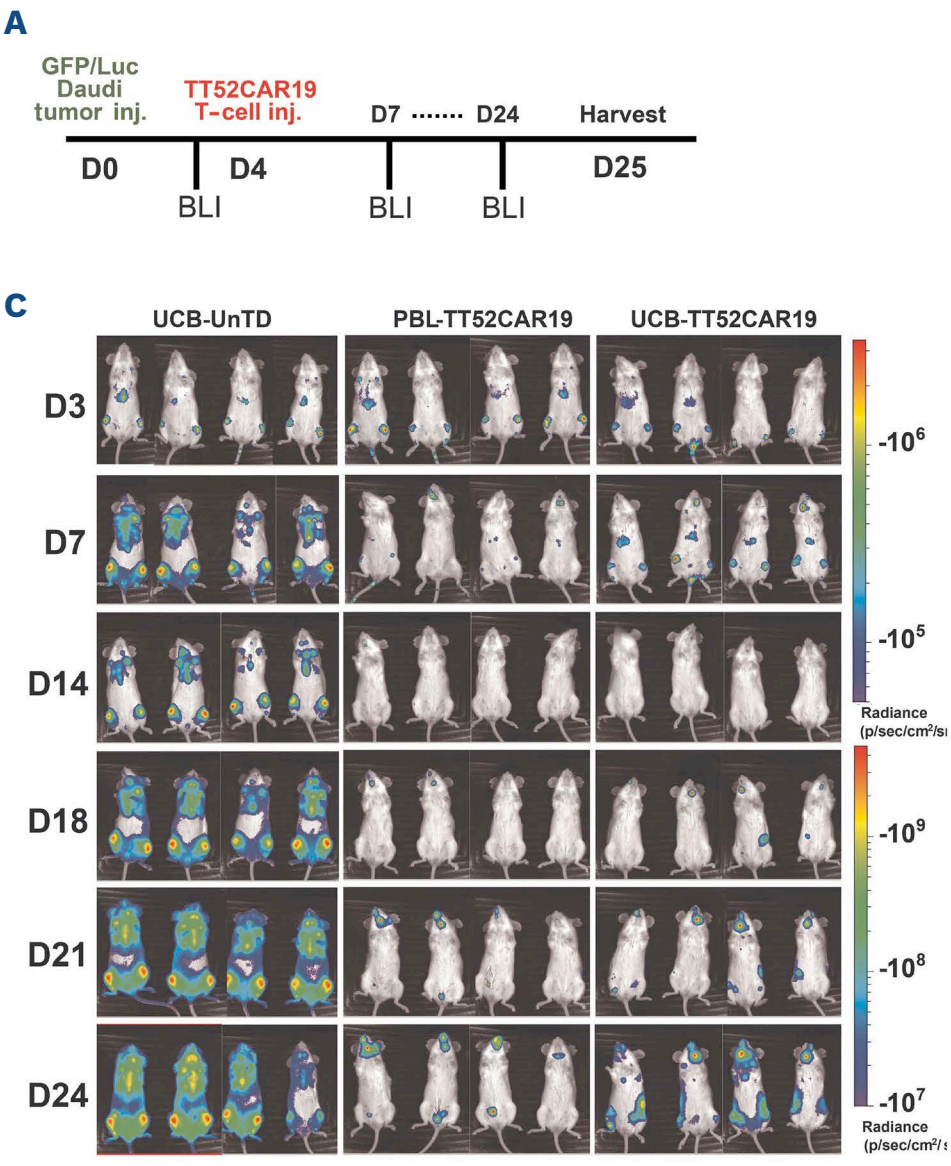

Figure 7. *In vivo* tumor clearance in human : murine xenograft model of CD19⁺ disease. Timeline of *in vivo* human:murine xenograft modeling indicating target and effector intravenous injection (inj.) days and bioluminescent imaging (BLI) time-points (A). Serial measurement of bioluminescence of Daudi CD19⁺ B-cell disease in immunodeficient NOD/SCID/γc (NSG) mice (N=12) infused with $5x10^5$ GFP/luciferase expressing Daudi CD19⁺ B cells were treated on day 4 with $5x10^6$ of either umbilical cord blood (UCB)-TT52CAR19 GMP1 (UCB1) (N=4) or peripheral blood lymphocyte (PBL) PBL-TT52CAR19 (N=4) and were monitored over a 4-week period (B, C). Non-transduced (UnTD) (N=4) T cells were used as controls. Error bars represent Standard Error of Mean (SEM). Significance compared by area under the curve using one-way ANOVA (F-value 35.86) with Tukey multiple comparison post-hoc; not significant (ns) $P \geq 0.05$, ****$P < 0.0001$.

CRISPR-Cas9 editing. Potential therapeutic applications include 'off the shelf' CAR T-cell therapies for ready access to products where autologous options are not available.

Disclosures

WQ, CG, RP, ASG and AE report that UCLB has filed intellectual property in relation to therapeutic cells (WO/2018/115887; PCT/GB2017/053862) and U6 minimal promoter (WO/ 2020/183197; PCT/GB2020/050651). UAM is a current employee of Miltenyi Biotec B.V. & Co. KG. WQ reports consultancy for Wugen, Novartis, Kite, Autolus, and Virocell & Galapagos. All other authors have no conflicts of interest to disclose.

Contributions

WQ is the principal investigator. CG, GO, LN, FS and WQ wrote the first draft of the manuscript. CG, AE, RP and WQ developed the vector configuration and genome editing strategy, and performed in vitro and in vivo phenotypic and functional assays. LN and UAM assisted with scalability of the platform. FS, HZ and PC manufactured the UCB-TT52CAR19 batches and performed the longitudinal stability tests. SAG and SA performed the molecular characterization of the final product. CG, GO, SAG and WQ analyzed the data and created the figures. All authors reviewed and approved the final version for publication.

Acknowledgments

We would like to thank Ailsa Greppi and Kyle O'Sullivan for their invaluable technical support with in vivo studies. Dr. Ayad Eddaudi at the UCL Joint Great Ormond Street Institute of Child Health and Institute of Ophthalmology Flow Cytometry Core Facility, supported by the Great Ormond Street Children's Charity (GOSHCC), grant reference U09822 (October 2007), UCL Capital Equipment Funding, School of Life and Medical Sciences (September 2012), and UK Research and Innovation, grant reference MR/ L012758/1 (March 2014). The Anthony Nolan Trust (803716/ SC038827) for their support and provision of healthy blood donations.

Funding

Supported by National Institute of Health Research (NIHR) and Great Ormond Street Biomedical Research Centre (RP-2014-05-007), BRC (IS-BRC-1215-20012) and Children with Cancer (2014/171), and by the Medical Research Council MR/X004619/1 and MRC Developmental Pathway funding scheme (DPFS). The views expressed are those of the author(s) and not necessarily those of the NHS, the NIHR or the Department of Health.

Data-sharing statement

All data and protocols associated with this work are

present in the paper or the Online Supplementary Appendix. The lentiviral plasmids generated in this study are available upon request from the corresponding author under a material transfer agreement. Raw NGS files were deposited in the NIH BioProject Database (BioProject accession n.: PRJNA1061060).

References

1. Maude SL, Laetsch TW, Buechner J, et al. Tisagenlecleucel in children and young adults with B-cell lymphoblastic leukemia. N Engl J Med. 2018;378(5):439-448.
2. Qayed M, McGuirk J, Myers G, et al. Leukapheresis guidance and best practices for optimal chimeric antigen receptor T-cell manufacturing. Cytotherapy. 2022;24(9):869-878.
3. Abecassis A, Roders N, Fayon M, et al. CAR-T cells derived from multiple myeloma patients at diagnosis have improved cytotoxic functions compared to those produced at relapse or following daratumumab treatment. EJHaem. 2022;3(3):970-974.
4. Brudno JN, Somerville RP, Shi V, et al. Allogeneic T cells that express an anti-CD19 chimeric antigen receptor induce remissions of B-cell malignancies that progress after allogeneic hematopoietic stem-cell transplantation without causing graft-versus-host disease. J Clin Oncol. 2016;34(10):1112-1121.
5. Zhang C, Wang XQ, Zhang RL, et al. Donor-derived CD19 CAR-T cell therapy of relapse of CD19-positive B-ALL post allotransplant. Leukemia. 2021;35(6):1563-1570.
6. Cruz CR, Micklethwaite KP, Savoldo B, et al. Infusion of donor-derived CD19-redirected virus-specific T cells for B-cell malignancies relapsed after allogeneic stem cell transplant: a phase 1 study. Blood. 2013;122(17):2965-2973.
7. Georgiadis C, Preece R, Nickolay L, et al. Long terminal repeat CRISPR-CAR-coupled "universal" T cells mediate potent anti-leukemic effects. Mol Ther. 2018;26(5):1215-1227.
8. Ottaviano G, Georgiadis C, Gkazi S, et al. Phase 1 clinical trial of CRISPR-engineered CAR19 universal T cells for treatment of children with refractory B cell leukemia. Sci Transl Med. 2022;14(668):eabq3010.
9. Qasim W, Zhan H, Samarasinghe S, et al. Molecular remission of infant B-ALL after infusion of universal TALEN gene-edited CAR T cells. Sci Transl Med. 2017;9(374):eaaj2013.
10. Benjamin R, Graham C, Yallop D, et al. Genome-edited, donor-derived allogeneic anti-CD19 chimeric antigen receptor T cells in paediatric and adult B-cell acute lymphoblastic leukaemia: results of two phase 1 studies. Lancet. 2020;396(10266):1885-1894.
11. Kagoya Y, Guo T, Yeung B, et al. Genetic ablation of HLA Class I, Class II, and the T-cell receptor enables allogeneic T cells to be used for adoptive T-cell therapy. Cancer Immunol Res. 2020;8(7):926-936.
12. Hu Y, Zhou Y, Zhang M, et al. Genetically modified CD7-targeting allogeneic CAR-T cell therapy with enhanced efficacy for relapsed/refractory CD7-positive hematological malignancies: a phase I clinical study. Cell Res. 2022;32(11):995-1007.
13. Webber BR, Lonetree CL, Kluesner MG, et al. Author Correction: Highly efficient multiplex human T cell engineering without double-strand breaks using Cas9 base editors. Nat Commun. 2019;10(1):5222.
14. Jo S, Das S, Williams A, et al. Endowing universal CAR T-cell with immune-evasive properties using TALEN-gene editing. Nat Commun. 2022;13(1):3453.
15. Iyer SP, Sica RA, Ho PJ, et al. The COBALT-LYM study of CTX130: a phase 1 dose escalation study of CD70-targeted allogeneic CRISPR-Cas9–engineered CAR T cells in patients with relapsed/refractory (R/R) T-cell malignancies. Hemasphere. 2022;6:163-164.
16. McGuirk J, Bachier CR, Bishop MR, et al. A phase 1 dose escalation and cohort expansion study of the safety and efficacy of allogeneic CRISPR-Cas9–engineered T cells (CTX110) in patients (Pts) with relapsed or refractory (R/R) B-cell malignancies (CARBON). J Clin Oncol. 2021;39(15_suppl):TPS7570.
17. Chiesa R, Georgiadis C, Syed F, et al. Base-edited CAR7 T cells for relapsed T-cell acute lymphoblastic leukemia. N Engl J Med. 2023;389(10):899-910.
18. Mold J, Venkatasubrahmanyam S, Burt T, et al. Fetal and adult hematopoietic stem cells give rise to distinct T cell lineages in humans. Science. 2010;330(6011):1695-1699.
19. Chiesa R, Gilmour K, Qasim W, et al. Omission of in vivo T-cell depletion promotes rapid expansion of naïve CD4+ cord blood lymphocytes and restores adaptive immunity within 2 months after unrelated cord blood transplant. Br J Haematol. 2012;156(5):656-666.
20. Liu E, Marin D, Banerjee P, et al. Use of CAR-transduced natural killer cells in CD19-positive lymphoid tumors. N Engl J Med. 2020;382(6):545-553.
21. Liu E, Tong Y, Dotti G, et al. Cord blood NK cells engineered to express IL-15 and a CD19-targeted CAR show long-term persistence and potent antitumor activity. Leukemia. 2018;32(2):520-531.
22. Shah N, Li L, McCarty J, et al. Phase I study of cord blood-derived natural killer cells combined with autologous stem cell transplantation in multiple myeloma. Br J Haematol. 2017;177(3):457-466.
23. Pegram H, Purdon T, van Leeuwen D, et al. IL-12-secreting CD19-targeted cord blood-derived T cells for the immunotherapy of B-cell acute lymphoblastic leukemia. Leukemia. 2015;29(2):415-422.
24. Riddell S, Sommermeyer D, Berger C, et al. Adoptive therapy with chimeric antigen receptor-modified T cells of defined subset composition. Cancer J. 2014;20(2):141-144.
25. Kwoczek J, Riese S, Tischer S, et al. Cord blood-derived T cells allow the generation of a more naïve tumor-reactive cytotoxic T-cell phenotype. Transfusion. 2018;58(1):88-99.
26. Sallusto F, Geginat J, Lanzavecchia A. Central memory and effector memory T cell subsets: function, generation, and maintenance. Annu Rev Immunol. 2004;22:745-763.
27. Kellner J, Yvon E, Parmar S. Ex vivo generation of umbilical cord blood T regulatory cells expressing the homing markers CD62L and cutaneous lymphocyte antigen. Oncotarget. 2018;9(72):33694-33701.
28. Kim D, Bae S, Park J, et al. Digenome-seq: genome-wide profiling of CRISPR-Cas9 off-target effects in human cells. Nat Methods. 2015;12(3):237-243.
29. Georgiadis C, Rasaiyaah J, Gkazi S, et al. Base-edited CAR T cells for combinational therapy against T cell malignancies. Leukemia. 2021;35(12):3466-3481.
30. Mock U, Hauber I, Fehse B. Digital PCR to assess gene-editing frequencies (GEF-dPCR) mediated by designer nucleases. Nat Protoc. 2016;11(3):598-615.
31. Mock U, Machowicz R, Hauber I, et al. mRNA transfection of a novel TAL effector nuclease (TALEN) facilitates efficient

knockout of HIV co-receptor CCR5. Nucleic Acids Res. 2015;43(11):5560-5571.
32. Qasim W. Genome-edited allogeneic donor “universal” chimeric antigen receptor T cells. Blood. 2023;141(8):835-845.
33. Martin KE, Hammer Q, Perica K, Sadelain M, Malmberg K-J. Engineering immune-evasive allogeneic cellular immunotherapies. Nat Rev Immunol. 2024;24(9):680-693.
34. Fraietta JA, Lacey SF, Orlando EJ, et al. Determinants of response and resistance to CD19 chimeric antigen receptor (CAR) T cell therapy of chronic lymphocytic leukemia. Nat Med. 2018;24(5):563-571.
35. Xu Y, Zhang M, Ramos C, et al. Closely related T-memory stem cells correlate with in vivo expansion of CAR.CD19-T cells and are preserved by IL-7 and IL-15. Blood. 2014;123(24):3750-3759.
36. Arcangeli S, Bove C, Mezzanotte C, et al. CAR T cell manufacturing from naive/stem memory T lymphocytes enhances antitumor responses while curtailing cytokine release syndrome. J Clin Invest. 2022;132(12):e150807.
37. Caël B, Galaine J, Bardey I, et al. Umbilical cord blood as a source of less differentiated T cells to produce CD123 CAR-T cells. Cancers (Basel). 2022;14(13):3168.
38. Taylor CJ, Peacock S, Chaudhry AN, Bradley JA, Bolton EM. Generating an iPSC bank for HLA-matched tissue transplantation based on known donor and recipient HLA types. Cell Stem Cell. 2012;11(2):147-152.
39. Xu H, Wang B, Ono M, et al. Targeted disruption of HLA genes via CRISPR-Cas9 generates iPSCs with enhanced immune compatibility. Cell Stem Cell. 2019;24(4):566-578.e7.